International Journal of Mechanical, Industrial and Aerospace Sciences
ISSN: 2517-9950
Vol:14, No:4, 2020

# Detection of Coupling Misalignment in a Rotor System Using Wavelet Transforms

Prabhakar Sathujoda

***Abstract*—**Vibration analysis of a misaligned rotor coupling bearing system has been carried out while decelerating through its critical speed. The finite element method (FEM) is used to model the rotor system and simulate flexural vibrations. A flexible coupling with a frictionless joint is considered in the present work. The continuous wavelet transform is used to extract the misalignment features from the simulated time response. Subcritical speeds at one-half, one-third, and one-fourth the critical speed have appeared in the wavelet transformed vibration response of a misaligned rotor coupling bearing system. These features are also verified through a parametric study.

***Keywords*—**Continuous wavelet transform, flexible coupling, rotor system, sub critical speed.

## I. Introduction

SHAFT misalignment is a condition in which the driving and driven machine shafts are not on the same centerline. It is a malfunction which induces additional reaction forces and moments on the shaft ends and is most common reasons for machine vibrations apart from rotor unbalance [1], which could also result in the failure of 60% to 70% rotating systems when the degree of misalignment is excessive [2], [3]. Hence it is essential to detect the coupling misalignment at any given time to avoid rotor failures. Perfect alignment between the driving and driven machines cannot be attained. Thus, a misalignment condition is virtually always present in the machine trains. Usually flexible couplings are used to accommodate the existing misalignment between driving and driven shafts and to transmit rotary power without torsional slip. Couplings can be classified as rigid, misalignment compensating, torsionally flexible or a combination as discussed in the paper by Rivin [4]. The effect of coupling geometry, mass, location and the coupling mass unbalance level on lateral vibrations of machines has been studied by Woodcock [5]. The additional forces and moments due to coupling misalignment for various types of couplings have been derived by Gibbons [6] and Sekhar and Prabhu [7].

Even though significant work has been done on couplings as reported in the review paper by Xu and Marangoni [8], not much literature is available on the vibration analysis of a misaligned rotor coupling system despite its importance in the industrial world. Al-Hussain [9] studied the dynamic stability of angular misaligned rigid rotors connected by a flexible coupling. Sekhar and Prabhu [7] have analyzed the dynamic behavior of a misaligned rotor-coupling bearing system using the higher order FEM. Patel and Darpe [10] analyzed the vibration characteristics of a misaligned rotor coupling system using FFT and rotor orbit data. Lei and et al. [11] proposed a diagnostic method to detect the misalignment based on the changes in rotor static and dynamic characteristics. Most of the previous works mainly focused on the vibration analysis of a misaligned rotor system using steady state response and frequency analysis. However, in case of engines which start and stop quite frequently such as aircraft and automobile engines, it is important to analyze the transient vibration response to detect coupling misalignment and estimate its severity before reaching the steady state. Few works are reported in this direction. Prabhakar et al. [12] analyzed the vibration response of a misaligned rotor coupling bearing system passing through the critical speed and found the continuous wavelet transform (CWT) is useful to extract the misalignment feature from the time response. Chadra and Sekhar [13] utilized short-time Fourier Transform (STFT), CWT and Hilbert-Huang transform to analyze the rotor faults including coupling misalignment. Recently, Zhiwei et al. [14] investigated the vibration features of an angular misaligned rotor coupling system using the smoothed pseudo Wigner-Ville distributions (SPWVDs).

Research works reported in references [12]-[14] mainly utilized the transient time response of the rotor system during coasting up/accelerating through the critical speed of the rotor system. Detection of coupling misalignment in a rotor coupling bearing system during coast down is rarely found in the literature, which is the subject of the interest of the present work. Transient analysis of a rotor-coupling-bearing system with shaft to shaft coupling misalignment and unbalance has been studied by using the FEM for flexural vibrations. A flexible coupling having a frictionless joint is considered in the analysis. CWT signal processing tool is implemented to extract is the misalignment features from the simulated time response of the rotor system when it is coasting down through the critical speed.

## II. Modelling of a Rotor-Coupling Bearing System

A rotor coupling bearing system shown in Fig. 1 (a) is considered in the present analysis. Dynamic modelling of a rotor bearing system using finite elements developed by Nelson and McVaugh [15] has been used in the present work, except flexible coupling. The typical shaft element without flexible coupling elements is shown in Fig. 1 (b). The element has two translational and two rotational degrees of freedom at each node represented by $q_1$ to $q_8$.

P. Sathujoda is professor at Department of Mechanical and Aerospace Engineering, Bennett University, India (e-mail: prabhakar.sathujoda@bennett.edu.in).

The modelling of flexible coupling, as discussed by Kramer [16], is utilized in the present study. A flexible coupling having a frictionless joint is considered in the study. For a frictionless radially stiff joint, the displacement at the two sides of the joint are identical and angles are different. Fig. 2 (a) shows the coordinates of the two shaft elements, which are to be joined. With $q_9 = q_5$ and $q_{10} = q_6$, the new coordinates are shown in Fig. 2 (b) for the elements when joined together. The stiffness matrix for this joint can be written as:

$$[K_{f1}] = \frac{EI}{l^3} \begin{matrix} [12][012][0-6l4l^2][6l004l^2][-1200-6l24\text{SYMMETRIC}] \\ [0-126l0024][0-6l-2l^200-6l-4l^2] \\ [6l002l^26l004l^2][00000006l4l^2][0000006l004l^2] \\ [000000-1200-6l12] \\ [0000000-126l0012][0000000-6l2l^200-6l4l^2] \end{matrix}$$

The equation of motion of the complete rotor system in a fixed co-ordinate system can be written as:

$$[M]\{\} + [D]\{\} + [K]\{q\} = \{Q\} \quad (1)$$

The stiffness matrix [K] in (1) considers the stiffness of the shaft elements including the coupling element and the bearing stiffness. The details of the [M] and [D] matrices of Equation (1) except for the coupling element are given in [15]. The external excitation matrix {Q} includes coupling misalignment and unbalance forces which are discussed in Section III.

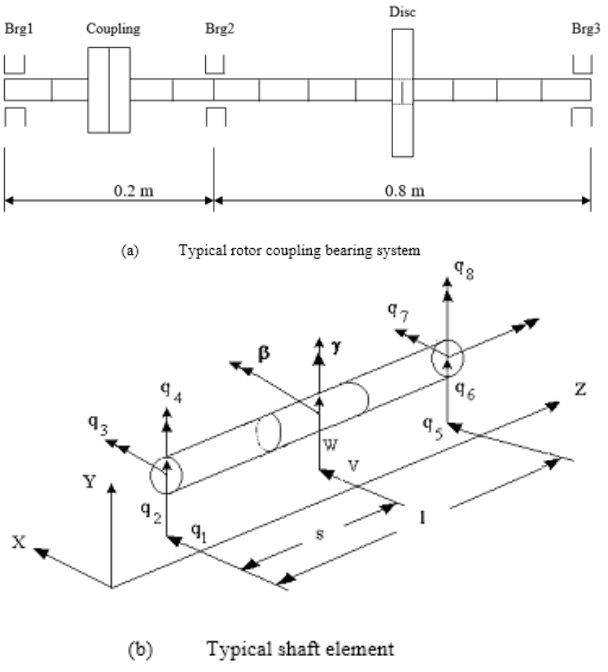


Fig. 1 Rotor-coupling-bearing system with typical finite rotor element and its co-ordinates

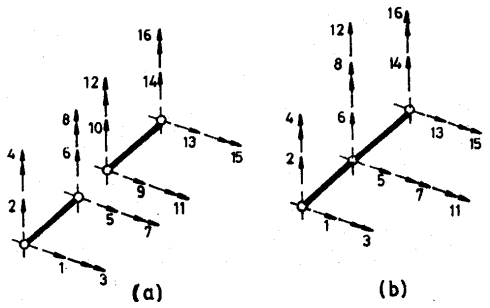


Fig. 2 Co-ordinates of two joined coupling elements

## III. Misalignment Forces

Additional forces and moments due to coupling misalignment, which are given in reference in [7], have been presented briefly here. Two misaligned shaft centerlines, Z1 and Z2 are shown in Fig. 3. The magnitude and the directions of displacements ΔX1, ΔY1, ΔX2 and ΔY2 can be obtained from the graphical plot of the reverse indicator readings. The misalignment forces and moments can be obtained using the following equation [7].

*Angular misalignment*:

$$\begin{gathered} MX1 = 0.0\ , MY1 = 0.0, MZ1 = Tq \quad / \quad \cos\theta \\ MX2 = -K_b\theta_3, MY2 = Tq\sin\theta_3, MZ2 = -Tq \\ FX1 = (-MY1 - MY2)/Z\,3, \\ FY1 = (MX1 + MX2)/Z\,3, \\ FZ1 = K_a\Delta Z + K_a \\ FX2 = -FX1, FY2 = -FY1, FZ2 = FZ1 \end{gathered}$$

The misalignment moments and the reaction forces would be acting as periodic loads on the rotating shafts with a periodic half-sinusoidal function having time period of $\pi/\omega$ as given in [7]. In the present work, $1\omega$, $2\omega$, $3\omega$ and $4\omega$ components of the reaction forces are considered for coupling misalignment. The reaction forces due to coupling misalignment are incorporated into the excitation matrix {Q} in the equation of motion (1) at the corresponding degrees of freedom, and these forces are given in (2) and (3):

$$\{Q_c^1\} = \begin{Bmatrix} FX1\sin\Omega t + FX1\sin 2\Omega t + FX1\sin 3\Omega t + FX1\sin 4\Omega t \\ FY1\cos\Omega t + FY1\cos 2\Omega t + FY1\cos 3\Omega t + FY1\cos 4\Omega t \\ 0 \\ 0 \end{Bmatrix} \quad (2)$$

$$\{Q_c^2\} = \begin{Bmatrix} FX2\sin\Omega t + FX2\sin 2\Omega t + FX2\sin 3\Omega t + FX2\sin 4\Omega t \\ FY2\cos\Omega t + FY2\cos 2\Omega t + FY2\cos 3\Omega t + FY2\cos 4\Omega t \\ 0 \\ 0 \end{Bmatrix} \quad (3)$$

where $\{Q_c^1\}$ and $\{Q_c^2\}$ are the nodal force vectors at the left and right side of the coupling. Apart from the misalignment forces, the unbalance forces at disc locations are considered in the analysis.

The force components in the x and y directions ($F_x$ and $F_y$) for an angular position $\theta$ are given as:

$$F_x = me\{\ddot{\theta}\sin\theta + \dot{\theta}^2\cos\theta\} \quad (4)$$

$$F_y = me\{-\ddot{\theta}\cos\theta + \dot{\theta}^2\sin\theta\} \quad (5)$$

where, *m* is the unbalance mass and e eccentricity.

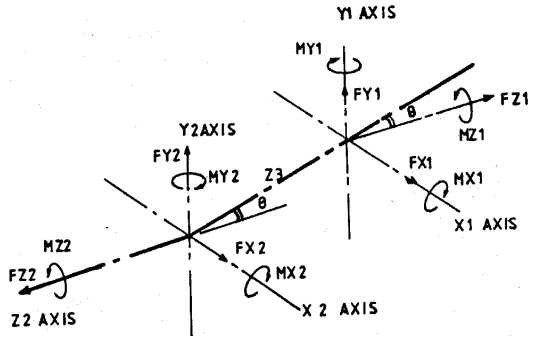


Fig. 3 Coupling co-ordinate system – Angular misalignment [6]

## IV. Results and Discussion

A rotor-coupling bearing system shown in Fig. 1 is considered when it is decelerating through its critical speed. The rotor system is discretized into 10 finite elements. The data used for the analysis are given in Table I. The first critical speed of the rotor system can be obtained by calculating the natural frequency of the rotor system using the eigenvalue problem and is found to be 1618 RPM [12]. Angular misalignment cases are analyzed in the present work. Time response is simulated by using the Houbolt time marching technique with a time step of 0.001s. The Morlet wavelet with a support length of (-4,4) is chosen for all the CWTs. The center frequency and bandwidth of the Morlet mother wavelet can be calculated, which in turn can be used for calculating the center frequency of the daughter wavelets using the scale.

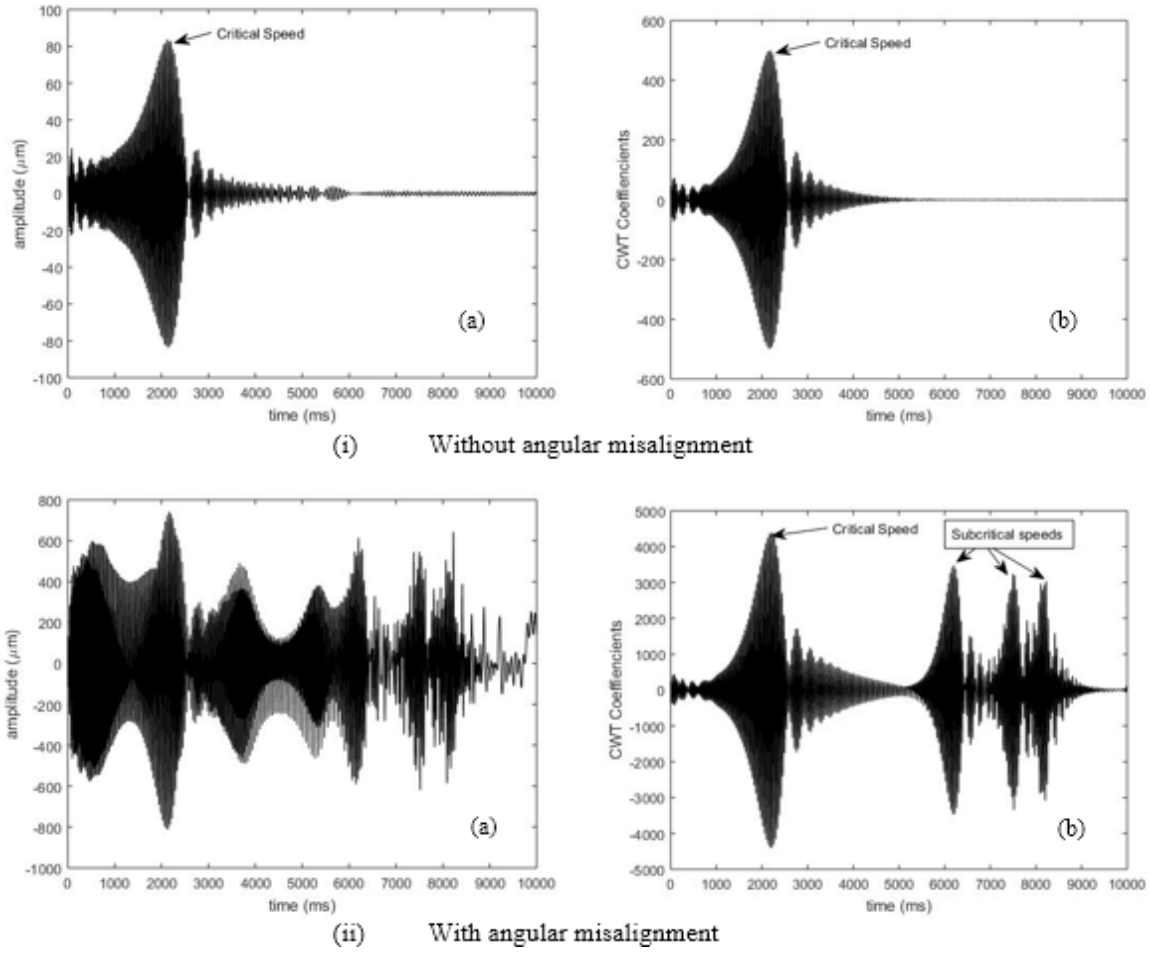


Fig. 4 Time response and corresponding CWT plots of a rotor-coupling bearing system (i) without misalignment (ii) with angular misalignment $\theta = 0.5^0$; when rotor is decelerating at -20 rad/s$^2$; (a) Time (b) CWT

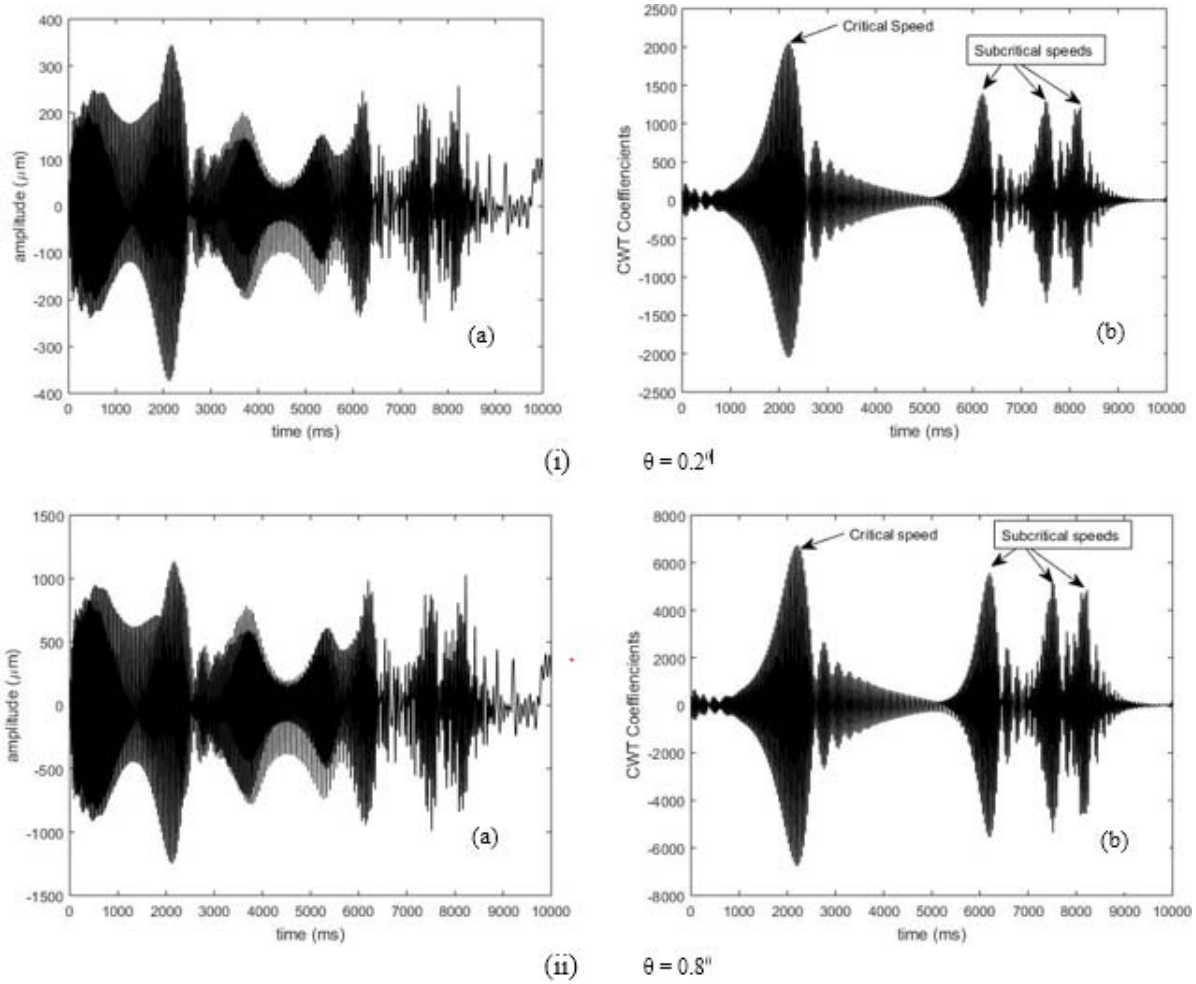


Fig. 5 Time response and corresponding CWT plots of a misaligned rotor-coupling bearing system (i) $\theta = 0.2^0$ (ii) $\theta = 0.8^0$; when rotor is decelerating at -20 rad/s$^2$; (a) Time (b) CWT

Transient time responses and the corresponding CWT plots of a rotor-coupling bearing with and without coupling misalignments are shown in Figs. 4-6. In all the cases, the time responses are simulated when the rotor system shuts-down at a speed of 200 rad/s (1910.8 RPM) and decelerating through its critical speed (1618 RPM). Hence the "zero" on time axis corresponds to 1910.8 RPM. Fig. 4 i (a) shows the time response of the rotor-coupling system when decelerating at -20 rad/s$^2$ without any misalignment. A peak at critical speed around 2 s, which corresponds to 1618 RPM (27 Hz), is evident from the time response. Time response is then transformed into wavelet domain using a scale of 35 and is plotted in Fig. 4 i (a). Again, a clear peak at critical speed can be found in the wavelet domain. However, when the misalignment is present, the critical speed peak cannot be identified easily from the time response and also apart from the critical speed peak, there are other peaks embedded in the time response as shown in Fig. 4 ii (a). A clear rise in the displacement amplitude can be noted when the misalignment is present, however, there are no specific symptoms of misalignment in the time response. Whereas the critical speed peak can be extracted using wavelet transform and can be clearly identified in Fig. 4 ii (b). Also, other peaks at one-half, one-third and one-fourth the critical speed can be identified in wavelet domain. These peaks appear when misalignment is present in the rotor system. The peaks at one-half, one-third and one-fourth the critical speeds can be extracted using the wavelet transforms and can be used to detect the coupling misalignment. Since the time signals captured during the shut-down process are nonstationary in nature, CWT can be used to extract the misalignment and to detect it.

A parametric study has been carried out for different angular misalignments and decelerations to further investigate the use of CWT for misalignment feature extraction. Fig. 5 shows the transient time response and the wavelet transformed plots of different misaligned rotors. There is a significant rise in vibration amplitude which can be observed from the time responses, however the misalignment features could not be identified in the time response for any values of angular misalignment (please refer to Figs. 5 i (a) and ii (a). The wavelet transformed plots are given in Figs. 5 i (b) and Fig. ii (b). Apart from the rise in the CWT coefficients, clear peaks at

critical speed, one-half, one-third and one-fourth the critical speed appear in the wavelet transformed time signals. Fig. 6 shows the time response and the corresponding CWT plots when the rotor is decelerating with -40 rad/s$^2$ and -80 rad/s$^2$.

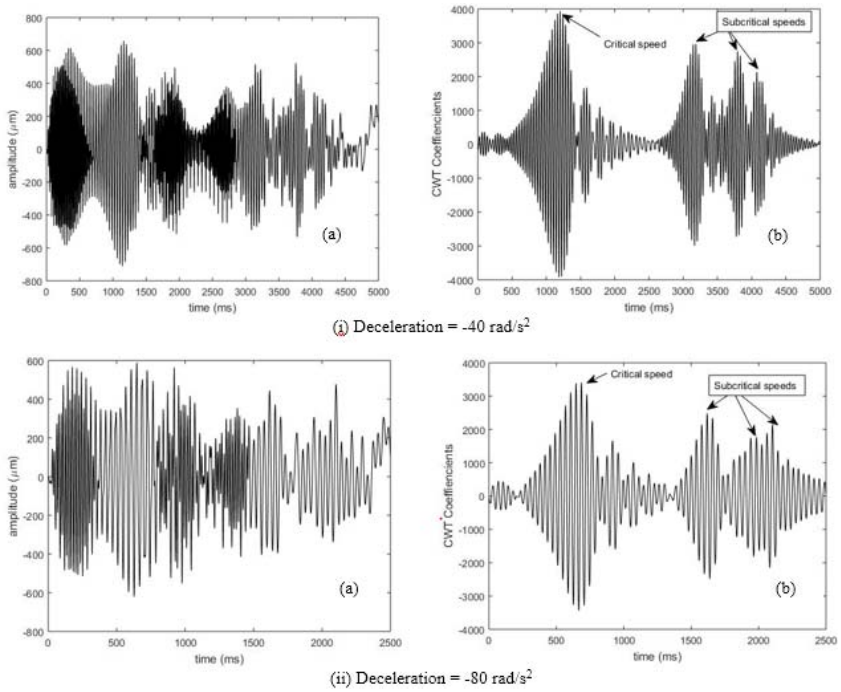


Fig. 6 Time response and corresponding CWT plots of a misaligned rotor-coupling bearing system for different decelerations ($\theta = 0.5^0$) (i) a = -40 rad/s$^2$ (ii) a = -80 rad/s$^2$; (a) Time (b) CWT

TABLE I
ROTOR-COUPLING -BEARING DATA

| Shaft | |
|---|---|
| Diameter, D | 20 mm |
| Density and Modulus of Elasticity | 7800 kg /m$^2$, 2.08 $10^{11}$ N/m$^2$ |
| Disc | |
| Mass, m | 5.5 kg |
| Polar moment of inertia, $I_P$ | 0.01546 kg-m$^2$ |
| Diametral moment of inertia, $I_D$ | 0.00773 kg-m$^2$ |
| Unbalance eccentricity, e | 0.008 mm |
| Coupling | |
| Type | diaphragm coupling |
| Outer diameter | 50 mm |
| Center of articulation, $Z_3$ | 75.15 mm |
| Bending spring rate per degree per disk pack, $K_b$ | 30 Nm/degree/disc pack |
| Bearing (isotropic) | |
| Stiffness | 2.5 $10^5$ N/m |
| Damping | 100 Ns/m |
| Angular Misalignment, θ | $0.1^0$ to $0.5^0$ |
| deceleration of the rotor, a | -20 rad/s$^2$ to - 80 rad/s$^2$ |
| Torque, Tq | 30 N-m |
| Critical speed of the rotor-coupling bearing system (frictionless joint coupling) | 1618 rpm (26.98 Hz) |

Similar to previous cases, the subcritical speed peaks appear in the CWT plots. When the rotor is decelerating with high decelerations such as -80 rad/s$^2$ in Fig. 6 (ii), there is a dip in the vibration amplitudes when compared to low angular deceleration. This is due to the reason that the time taken to pass the critical speed is long when the rotor is decelerating with low angular decelerations. From this study, a CWT can be used as an effective tool to extract the coupling features from time response when the rotor is decelerating through critical speed.

## V. CONCLUSION

The transient response of a misaligned rotor coupling bearing system while decelerating through critical speed has been analyzed by using FEM for flexural vibrations and CWT. A coupling having a frictionless joint is considered with angular misalignment. The coupling misalignment features such as peaks at one-half, one-third and one-fourth the critical speed can be extracted from the transient time response of a rotor-coupling bearing system using CWT. A parametric study for different angular misalignments and decelerations has been performed to support the present study. The analysis shows that the CWT can be used as a signal processing tool for detecting the coupling misalignment while the rotor coupling bearing system is decelerating through the critical speed.

## REFERENCES

[1] Piotrowski, J. Shaft Alignment Handbook, third ed., CRC Press, Ohio, 2006.
[2] Sinha JK, Lees AW and Friswell MI. Estimating unbalance and misalignment of a flexible rotating machine from a single run-down. J Sound Vib 2004; 272: 967–989.

[3] Fei, C., Fengrui, B., Chao, C., Song, W., and Heng, Z. Research on double span rotor system driven by motorized spindle with coupling misalignment, Advances in Mechanical Engineering (2019) 11(4), 1–17.
[4] Rivin, E. I. Design and application criteria for connecting couplings. Trans. ASME, J. Mechanisms, Transm. Automn Des., 1986, 108, 96-104.
[5] Woodcock, J. S. The effect of couplings upon the vibrations of the rotating machinery. In Proceedings of International Conference on Flexible Couplings, University of Sussex, Brighton, 1977, pp. E-1-1 - E-1-20 (Michael Neale and Associates Limited).
[6] Gibbons, C. B. Coupling misalignment forces. In Proceedings of 5th Turbomachinery Symposium, Gas Turbine Laboratories, Texas A&M University, Texas, 1976, 111-116.
[7] Sekhar, A. S. and Prabhu, B. S. Effects of coupling misalignment on vibrations of rotating machinery. J. Sound Vibr., 1995, 185(4), 655-671.
[8] Xu, M. and Marangoni, R. D. Vibration analysis of a motor flexible coupling rotor system subjected to misalignment and unbalance, Part I: theoretical model and analysis. J. Sound Vibr., 1994, 176(5), 663-679.
[9] Al-Hussain KM. Dynamic stability of two rigid rotors connected by a flexible coupling with angular misalignment. J Sound Vib 2003; 266: 217–234.
[10] Patel, T.H. and Darpe, A.K. Experimental investigations on vibration response of misaligned rotors, Mech. Syst. Sig. Process. 2009, 23, 2236–2252.
[11] Qu, L., Lin, J., Liao, Y., & Zhao, M. Changes in rotor response characteristics based diagnostic method and its application to identification of misalignment. Measurement 2019, 138, 91-105.
[12] Prabhakar, S., Sekhar, A.S., and Mohanty, A.R. Vibration analysis of a misaligned rotor-coupling-bearing system passing through the critical speed. J Mech Eng Sci 2001, 215, 1417–1428.
[13] M.C.S. Reddy, M.C.S. and Sekhar, A.S. Detection and monitoring of coupling misalignment in rotors using torque measurements, Measurement 2015, 61, 111–122.
[14] Liu, Z., Wu, K., Ma, Z. et al. Vibration Analysis of a Rotating Flywheel/Flexible Coupling System with Angular Misalignment and Rubbing Using Smoothed Pseudo Wigner–Ville Distributions. J. Vib. Eng. Technol. (2019): http://doi-org-443.webvpn.fjmu.edu.cn/10.1007/s42417-019-00189-y.
[15] Nelson,,H. D. and McVaugh, J. M. The dynamics of rotor bearing systems using finite elements. Trans. ASME, J. Engng for Industry, 1976, 98(2), 593-600.
[16] Kramer, E. Dynamics of Rotors and Foundations, pp. 224 - 226 (Springer-Verlag, Berlin).